JGP Journal of General Physiology

COMMUNICATION

Contraction–relaxation coupling is unaltered by exercise training and infarction in isolated canine myocardium

Farbod Fazlollahi, Jorge J. Santini Gonzalez, Steven J. Repas, Benjamin D. Canan, George E. Billman, and Paul M.L. Janssen

The two main phases of the mammalian cardiac cycle are contraction and relaxation; however, whether there is a connection between them in humans is not well understood. Routine exercise has been shown to improve cardiac function, morphology, and molecular signatures. Likewise, the acute and chronic changes that occur in the heart in response to injury, disease, and stress are well characterized, albeit not fully understood. In this study, we investigated how exercise and myocardial injury affect contraction–relaxation coupling. We retrospectively analyzed the correlation between the maximal speed of contraction and the maximal speed of relaxation of canine myocardium after receiving surgically induced myocardial infarction, followed by either sedentary recovery or exercise training for 10–12 wk. We used isolated right ventricular trabeculae, which were electrically paced at different lengths, frequencies, and with increasing β-adrenoceptor stimulation. In all conditions, contraction and relaxation were linearly correlated, irrespective of injury or training history. Based on these results and the available literature, we posit that contraction–relaxation coupling is a fundamental myocardial property that resides in the structural arrangement of proteins at the level of the sarcomere and that this may be regulated by the actions of cardiac myosin binding protein C (cMyBP-C) on actin and myosin.

Introduction

A strong and forceful contraction of the heart is essential to provide adequate cardiac output. The duration of this contraction phase needs to be sufficiently long to eject most of the blood from the heart into the arterial system. In humans with systolic dysfunction, myocardial force typically develops more slowly and results in incomplete ejection of ventricular blood. When this reduced ejection fraction becomes critically low, end-stage heart failure ensues—a debilitating disease affecting >6.2 million Americans and resulting in an estimated annual national health care burden of $30.7 billion (Savarese and Lund, 2017).

A fast relaxation is needed to refill the ventricles with blood rapidly for the subsequent heartbeat. With increasing heart rate, the force and rate of myocardial contraction increases. However, a proportionally compensatory increase in the rate and magnitude of myocardial relaxation must also occur simultaneously (Janssen and Periasamy, 2007). When there is a mismatch in these rates and forces, the heart is physically unable to fill adequately and thereby is unable to eject enough blood to the tissues to maintain oxygenation, regardless of the ability to contract appropriately. This is termed diastolic dysfunction, or heart failure with preserved ejection fraction, and is frequently a precursor to systolic heart failure, wherein the heart cannot contract adequately (Borlaug and Kass, 2008; Dorhout Mees, 2013; Janssen and Periasamy, 2007).

Ideally, the heart rapidly develops sufficient pressure to open the aortic valve, sustains pressure to eject most of the ventricular volume, and subsequently relaxes rapidly. Past analyses on twitch contractions in murine and rat myocardium showed a tight coupling between the maximal rate of force development (dF/dt) and the maximal rate of force decline (−dF/dt; Hiranandani et al., 2007; Janssen et al., 2005; Stull et al., 2006, 2002). With contraction and relaxation coupled to each other in the myocardium, any changes in contractility would be automatically met with a proportionate change in relaxation to maintain cardiac output any time the oxygen demands of the body change. If this is a fundamental property of myocardium, then any intervention that prolongs and enhances contractile force would also prolong relaxation, compromising adequate refilling, particularly at higher heart rates. Likewise, hastening relaxation would be beneficial for filling, but this would imply a

Department of Physiology and Cell Biology, College of Medicine, Ohio State University, Columbus, OH.

Correspondence to Paul M.L. Janssen: janssen.10@osu.edu

This work is part of a special collection on myofilament function and disease.

hastening of pressure development or its maintenance, thereby reducing ejection fraction.

Whether or not contraction and relaxation are intimately coupled in larger mammals is critical to know but incompletely understood. There are many key differences between the human heart and the murine heart that make side-by-side physiological comparisons and subsequent clinical translation difficult, if not altogether inappropriate. In addition to the 10-fold higher resting heart rate in mice as compared with that of humans, mice also have a 10-fold faster motoneuron action potential duration (30 versus 300 ms in humans; Janssen et al., 2016). Mice predominantly express the α-myosin heavy chain, which is fivefold faster than the β-myosin heavy chain predominantly expressed in humans and other large mammals (Jones et al., 1996). The murine heart also cycles only 3% of its non-SR calcium content compared with 30% in the human heart. Finally, the murine heart's contractile kinetics is approximately fivefold faster than that of humans and its contractile reserve is fivefold smaller. Because most of these differences are based on the high heart rate in mice, animal models with a heart rate more comparable to humans, such as dogs, sheep, and pigs, should have a much more human-like contraction–relaxation (CR) coupling profile.

It is also critical to understand if disease alters CR coupling. Over the course of cardiac disease development, myriad changes occur within the tissue. Metabolic perturbations, changes in gene expression, posttranslational protein modifications, and many other phenomena take place at the advent of disease and continue through the course of disease, ultimately resulting in tissue remodeling that is often permanent in terminally differentiated tissues, such as the heart (Bertero and Maack, 2018). In the case of a myocardial infarction (MI), a portion of the myocardium is starved of blood supply long enough for that hypoxemic tissue to die, after which the tissue undergoes necrosis and scar formation (Ma et al., 2014). The resulting scar has lost all metabolic and contractile capacity and merely serves as a space-filling bridge for healthy myocardium (Anversa et al., 1991; Weber et al., 1990). In the case of heart failure, the prolonged stresses placed on the heart through secondary mechanisms such as hypertension, diabetes, obesity, drug abuse, and infarctions lead to different forms of remodeling depending on the causative factor. This remodeling can take the form of fibrotic stiffening, concentric hypertrophic thickening, overstretching and eccentric hypertrophy, fatty infiltration, and many others, all of which alter the overall function of the heart and could easily affect the relationship between contraction and relaxation (Kessler et al., 2014).

Likewise, improved function is often seen with exercise training, yet whether CR-coupling is changed in trained subjects is also unknown. To cope with increased oxygen and nutrient needs of the body during exercise, many acute changes occur in the heart. HR increases, end-diastolic volume increases, systolic volume increases, β-adrenoceptor response increases, contractility increases, and refractory period decreases. Routine exercise over an extended period leads to these acute changes causing compensatory remodeling within the myocardium, resulting in resting bradycardia, electrocardiographic changes, and metabolic changes in line with increased efficiency with oxygen, glucose, fat, and ATP utilization. Long-term consistent exercise has been shown to elicit a concentric cardiac hypertrophy, making the tissue more densely muscular without the harmful sequelae of concentric hypertrophy secondary to hypertension (Billman et al., 2015; Gielen et al., 2015; Ritzer et al., 1980; Vega et al., 2017). Again, these changes occur at both the molecular and tissue level and could potentially alter CR interplay. We have previously shown that exercise training led to a significant increase in developed force (F_{dev}), time to peak tension (TTP), and time to both 50% and 90% relaxation (RT50 and RT90, respectively) across all conditions (length, frequency, and isoproterenol), when compared with sedentary animals. MI, conversely, led to either no change or a decrease in F_{dev} in exercise-trained animals compared with MI sedentary (MIS) animals. These differences in contractile function are also evident in the range of dF/dt, which is reduced in the MI groups (no more than 400 mN/mm^2/s), whereas this is over 600 mN/mm^2/s in the non-MI groups.

In the present study, we investigate the effect of exercise- and/or injury-mediated remodeling on CR coupling in a canine model via retrospective analysis of myocardial twitch contractions. These data allowed us to study CR coupling in large mammals with heart rates comparable to humans in a controlled environment and, importantly, to study changes in CR coupling with common sources of cardiac remodeling: exercise and MI.

Materials and methods

All animal procedures were approved by the Ohio State University Institutional Animal Care and Use Committee and conformed to the Guide for the Care and Use of Laboratory Animals published by the U.S. National Institutes of Health (NIH publication no. 85–23, revised 1996). Data were collected during multiple previous studies (Billman et al., 2010; Billman and Harris, 2011; Billman and Kukielka, 2008; Bonilla et al., 2012; Hiranandani et al., 2010; Kukielka et al., 2011) but had not yet been analyzed or used in those publications. Muscle contraction profiles from n = 40 animals were used in the analysis. Details on the experimental design, animal source, training scheme, and cardiac trabeculae dissection were previously described (Billman, 2006, 2005; Billman et al., 2010; Canan et al., 2016). Overall, data from n = 13 control sedentary (CS), n = 13 control trained (CT), n = 8 MIS, and n = 6 MI trained (MIT) dogs were used, with MI and exercise protocols previously described in more detail (Billman et al., 2006; Billman and Kukielka, 2007, 2006).

Briefly, small linear multicellular muscle preparations were dissected from the right ventricular free wall. These muscle preparations were mounted in an experimental chamber in which length of the muscle could be changed and pacing frequency controlled. Experiments were performed at 37°C with superfusion of Krebs–Henseleit solution (137 mM NaCl, 5 mM KCl, 0.25 mM $CaCl_2$, 20 mM $NaHCO_3$, 1.2 mM NaH_2PO_4, 1.2 mM $MgSO_4$, and 10 mM dextrose) bubbled with a gas mixture of 95% O_2 and 5% CO_2. Routinely, more than one muscle was assessed for each dog (up to seven per dog), and no more than four muscles per dog were included in the analysis.

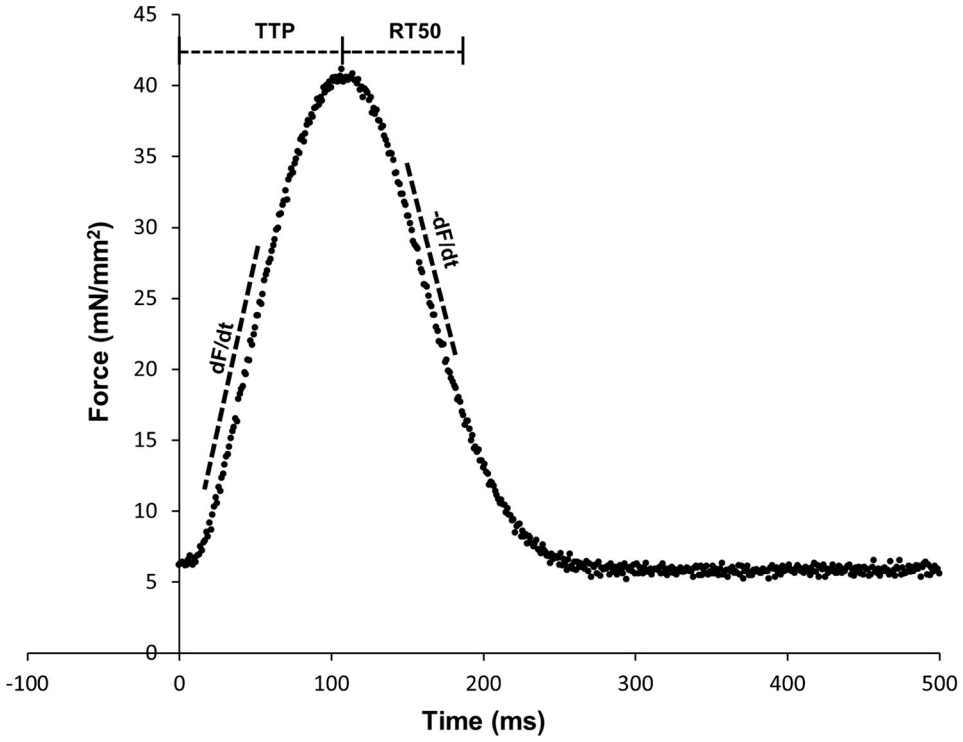

Figure 1. **Schematic of how calculations of dF/dt, −dF/dt, TTP, and RT50 were made in the analysis of twitch data.** Data shown were recorded from canine right ventricular trabecula, plotting F_{dev} (normalized to cross-sectional area assuming ellipsoid shape of muscle, in millinewtons per square millimeter) versus time (in milliseconds). Example tangent lines used to calculate dF/dt and −dF/dt are shown. The length of time from the initiation of the twitch contraction to the maximal F_{dev} is the TTP. The length of time from the peak F_{dev} to 50% of the peak F_{dev} is the RT50.

Once equilibrated, optimal length/preload was determined by stretching the mounted muscle while stimulating at 1 Hz until additional stretching would not result in an increased active F_{dev}. Data from each muscle were obtained first at baseline (1 Hz, optimal preload), then at four different lengths near end-systolic length: 85% of optimal length, then at 90%, 95%, and 100% of optimal length, with time for equilibration at each length before data acquisition. At each experimental condition, the muscle was allowed to equilibrate for ∼2–3 min before taking measurements and moving on to the next condition. Thereafter, the muscles were paced at 1, 2, 3, 4, and 5 Hz to encompass the entire in vivo range of heart rates for the canine. Lastly, a concentration–response curve for isoproterenol, a β-adrenoceptor agonist (CAS number 51-31-0; Sigma-Aldrich) was performed from 10^{-9} to 10^{-6} M, in semilog steps. From each twitch contraction, the maximal rise of force (+dF/dt) and maximal decline of force (−dF/dt) were assessed using custom-written software (LabView; National Instruments), with the magnitude of force normalized to cross-sectional area of the muscle (assuming ellipsoid shape). −dF/dt was calculated as the maximum derivative of the force decline by plotting the first derivative of force and finding the lowest point of this curve. This maximal rate of force decline consistently occurs around the time that force has declined to ∼50%. Likewise, +dF/dt was calculated as the maximum derivative of the force incline by plotting the first derivative of force and finding the highest point of this curve. This maximal rate of force development consistently occurs around the time that force is ∼50% of the maximal F_{dev}. TTP was calculated as the length of time from stimulation to maximal F_{dev}. RT50 was calculated as the length of time from peak F_{dev} to 50% of its value. Derivation of these values is described in a schematic in Fig. 1.

Data were tabulated and plotted, and then Pearson correlation coefficients were calculated using KaleidaGraph software (v4.5; Synergy Software). The statistical comparisons that directed the present work were described previously (Canan et al., 2016) and used a two-factor mixed-design ANOVA with or without inclusion of a repeated-measures variable. Post hoc comparisons were made using the Tukey–Kramer multiple-comparison test.

Results

Length-dependent activation

Increasing muscle length consistently resulted in a significantly increased F_{dev}, in agreement with previous work (Canan et al., 2016). The first derivative of the rate of change of F_{dev} with respect to time was calculated for force increasing to peak tension (contraction = dF/dt) and for force decreasing to 50% of peak tension (relaxation = −dF/dt) for each muscle. Data from a representative animal in the CS group were plotted with dF/dt on the abscissa and −dF/dt on the ordinate to illustrate the linearity of correlation between these variables (Fig. 2 A). The Pearson correlation coefficient for this relationship was calculated as $R^2 = 0.981$.

Force–frequency relationship

For each muscle, at optimal length, the frequency of stimulation was increased from 1 to 5 Hz in 1-Hz increments, and dF/dt and

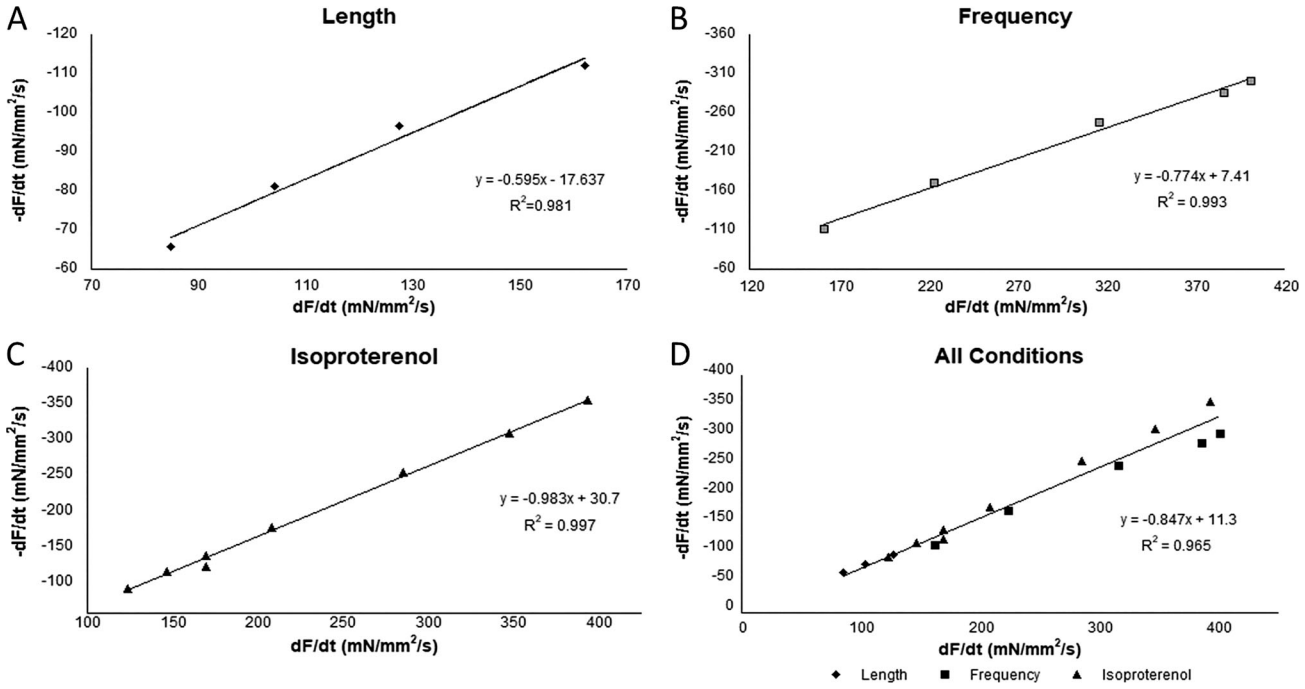

Figure 2. **Data presented were from one dog in the CS group. (A)** The results from the length-dependent activation experiment show strong linear correlation between CR rates, with a Pearson coefficient of R^2 = 0.981. **(B)** The results from the frequency-dependent activation experiment show a strong linear correlation for CR, R^2 = 0.993. **(C)** These data show that the results of the isoproterenol dose–response experiment have a strong linearity, with R^2 = 0.997. **(D)** Combination of all three experiments into one plot showing a tight linear correlation for all cardiac output regulatory mechanisms at R^2 = 0.965. Linear regression and Pearson correlation coefficient are calculated as shown.

–dF/dt were calculated at each step. Increasing stimulation frequency consistently resulted in an increased F_{dev}, in agreement with previous work (Canan et al., 2016). Data from a representative animal were plotted with dF/dt versus –dF/dt (Fig. 2 B). The Pearson correlation coefficient for this relationship was calculated as R^2 = 0.993.

β-Adrenergic stimulation

At optimal length and 1-Hz stimulation, each muscle was exposed to increasing concentrations of isoproterenol. The F_{dev} increased, while TTP and RT50 decreased proportionally as the isoproterenol dose increased. At each concentration of isoproterenol, dF/dt and –dF/dt were again calculated and plotted against each other for a representative animal from the CS group (Fig. 2 C). The Pearson correlation coefficient for this relationship was calculated as R^2 = 0.997.

All data from the above three analyses were plotted on shared axes (dF/dt versus –dF/dt; Fig. 2 D). In nearly all situations, F_{dev} and dF/dt changes occur in parallel. This occurs because the magnitude of the F_{dev} component change is nearly always greater than that of the kinetic component, and thus the impact of F_{dev} on the change in dF/dt is in the same direction. For nearly all conditions, the percentage change of F_{dev} is greater than that of the kinetic changes, and thus the ΔF_{dev} dominates the ΔdF/dt. These data demonstrate that, despite the activation of different biochemical and physiological regulatory mechanisms, the interplay between contraction and relaxation persists, and the two remain similarly correlated. The collective Pearson correlation coefficient was calculated as R^2 = 0.965.

Overall correlations

To demonstrate the linearity of correlation between contraction and relaxation, dF/dt and –dF/dt values from the force–frequency relationship, length-dependent activation, and β-adrenergic response protocols from all muscles analyzed for each dog in each group were averaged. Then for each group, all dog averages were averaged to create a single coordinate (weighted average dF/dt and weighted average –dF/dt) for each experimental group. The data from the CS, CT, MIS, and MIT animals were plotted (Fig. 3, A–D, respectively). The Pearson correlation coefficient for the average CR relationship for each group was calculated as follows: CS, R^2 = 0.997; CT, R^2 = 0.996; MIS, R^2 = 0.997; and MIT, R^2 = 0.997. Analysis of each of the three experimental conditions (length, frequency, and isoproterenol) showed that the ratio between –dF/dt and dF/dt was constant. Overall, this ratio was 0.786 for all the length data, 0.758 for all the frequency data, and 0.752 for all the isoproterenol data across all groups, with no significant difference between groups.

To eliminate the possibility that the perceived coupling between contraction and relaxation is due to a scaling with peak force, the kinetics of contraction and relaxation were determined considering only the TTP and RT50, respectively. Weighted averages for TTP and RT50 for each experimental group were calculated as described above by obtaining a collective average of TTP and RT50 for all muscles analyzed for each dog, then data combined from all dogs in each group were collectively averaged to obtain a single 2-D array for each group. All four arrays were plotted on shared axes, and a Pearson

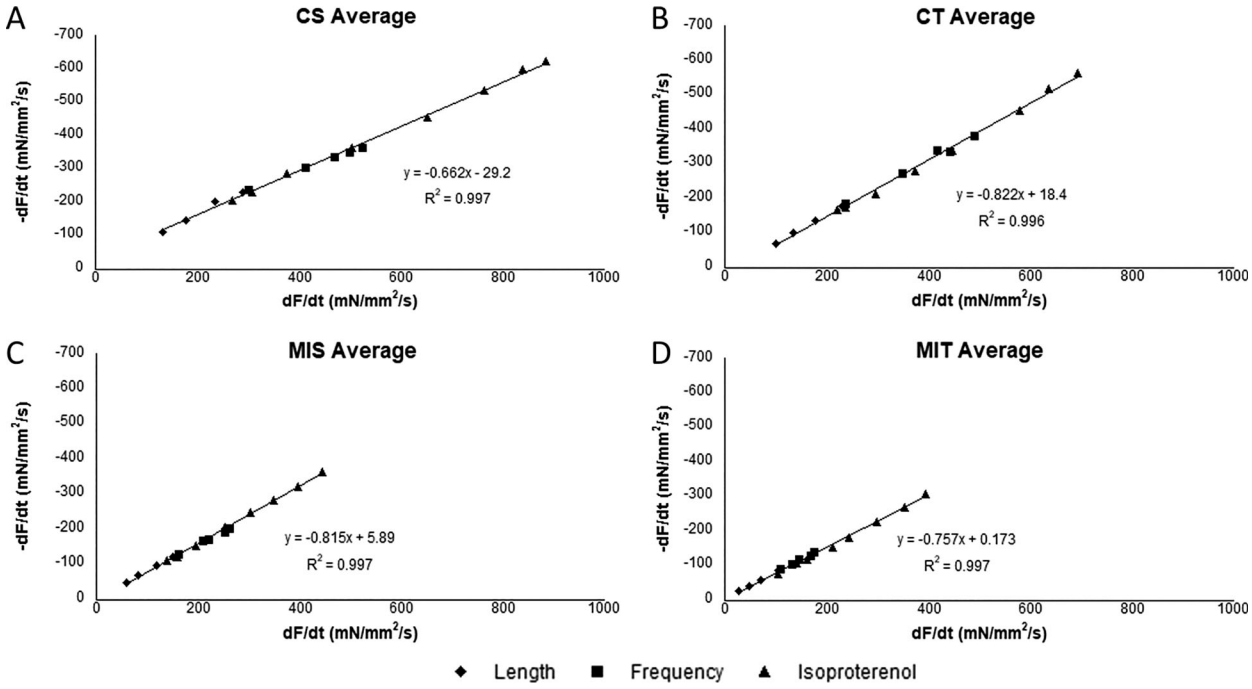

Figure 3. **Weighted average of data across all animals within each experimental group for length-dependent activation, frequency-dependent activation, and β-adrenergic stimulation measurements, testing all three cardiac output regulatory mechanisms. (A)** Data from the CS group show strong correlation across all three cardiac output regulatory mechanism tests at R^2 = 0.997. **(B)** Data from the CT group show tight correlation at R^2 = 0.996. **(C)** Data from the MIS group show tight correlation, with R^2 = 0.997. **(D)** Data from the MIT group show tight linear correlation, with R^2 = 0.997. Linear regression and Pearson correlation coefficient are calculated as shown.

correlation coefficient of 0.943 was calculated (Fig. 4), demonstrating that CR coupling is not due to scaling.

Discussion

The present study investigated CR coupling in canine myocardium with or without exercise training and MI. We have previously shown that exercise training leads to a significant increase in TTP, RT50, and RT90 across all conditions (length, frequency, and isoproterenol), when compared with sedentary animals. MI, conversely, leads to either no change or a decrease in F_{dev} in exercise trained animals compared with MIS animals. These differences in contractile function are also evident in the range of dF/dt, which is reduced in the MI groups (no more than 400 mN/mm²/s), but >600 mN/mm²/s in the non-MI groups (Canan et al., 2016). After assessing contraction and relaxation rates using the three main mechanisms of cardiac output regulation (length-dependent activation, frequency-dependent activation, and β-adrenergic stimulation), we found that in all three situations, contraction and relaxation show tight linear correlation (Fig. 2). Of note and completely novel is that the linearity persists regardless of experimental group (Fig. 3). As such, our results demonstrate that whether at baseline conditions, after exercise training, or after permanent ischemic damage, contraction and relaxation are intimately coupled in canine myocardium.

These findings demonstrate that persistent coupling of contraction and relaxation, despite damage and remodeling, is not dependent on macro-architecture. In addition, since these observations were made ex vivo, disconnected from the nervous system and systemic circulation, CR coupling must be a quality present in the myocardial tissue itself. Furthermore, while our study was conducted under isometric ex vivo conditions, CR coupling is still seen with respect to exercise in vivo in the canine model, as demonstrated by Mannozzi et al. (2020). Therefore, the mechanism for CR coupling must be at the level of the myocyte (Allen and Kurihara, 1979; Backx et al., 1995; Janssen, 2019; Janssen et al., 2002; Milani-Nejad et al., 2013; Monasky et al., 2008), the regulation of which must occur in brief efficient steps to keep up with rapid changes in cardiac demand.

Prior studies by our group and others have shown that when the ratio of the rates of cardiac contractile force generation and relaxation are calculated in various murine models, contraction and relaxation are consistently linearly correlated. Model systems exhibiting either ∼40% reduction of expression of SERCA (resulting in impaired transfer of Ca^{2+} to the SR and a slower calcium transient; Periasamy et al., 1999) or expression of the faster 1a isoform of SERCA (resulting in a faster calcium transient; Loukianov et al., 1998) both showed CR coupling similar to that of control mice. These results were demonstrated again after analysis of Duchenne's muscular dystrophy model (*mdx* mice; Janssen et al., 2005), LAMP-2 deficient model (Stypmann et al., 2006), sarcolipin overexpression and knockout models (Babu et al., 2006), and C57BL/6, C57BL10, and FVBN mouse strains (Janssen, 2010). The only mutation to exhibit a change in the slope of the correlation between dF/dt and –dF/dt has been cardiac myosin binding protein C (cMyBP-C) truncation,

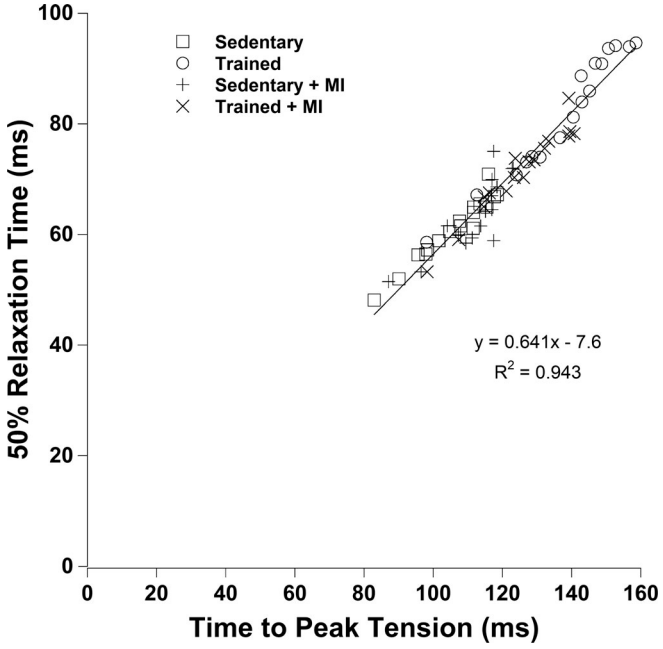

Figure 4. **Plot of TTP versus RT50.** Values were calculated as the weighted averages from all three experimental protocols (length, frequency, and β-adrenergic stimulation). Regardless of the experimental group to which the animals belong, TTP (as a surrogate for contraction) and RT50 (as a surrogate for relaxation) remain tightly correlated, with an overall Pearson coefficient of 0.943. These results demonstrate that CR coupling persists when contraction and relaxation kinetics are determined from contraction and relaxation times and not a scaling of relaxation with peak force.

resulting in nonfunctional cMyBP-C expression (Palmer et al., 2004). In a quantitative comparison of the slopes of the CR relationship, both rodents and canines, with exception of the cMyBP-C mouse, were virtually identical (near 0.8).

The cMyBP-C mutants showed a significant 32% decrease in the slope of the correlation between dF/dt and −dF/dt when compared with normal littermates, where the correlation itself was as strong (by R^2) as in other strains. Put another way, the intimate relationship between contraction and relaxation persists in cMyBP-C mice, but a given change in contractile rate results in a 32% proportionately smaller change in relaxation rate (and vice versa) compared with normal littermates, which physiologically corresponds to a less robust change in relaxation rate in response to a given increase in contractile rate. This shows that cMyBP-C plays a role in the efficiency of CR coupling.

MyBP-C has been shown to exist in the C-zones of the A band within the sarcomeric complex and has been shown to interact directly with actin filaments by electron tomography in intact frog sartorius (Craig and Offer, 1976; Heling et al., 2020; Luther et al., 2011). Specifically, the cardiac isoform has been shown to contain an extra N-terminal domain (C0, region absent in skeletal isoforms), multiple phosphorylation sites, and a 28–amino acid loop in the C5 domain (Gautel et al., 1995; Yasuda et al., 1995). The N-terminal domain cooperatively activates/inhibits the thin and thick filament, thereby directly modulating contraction and relaxation (Risi et al., 2018). The complete mechanism and details of cMyBP-C's role in CR coupling is incompletely understood, but based on our work and the current available literature, we speculate CR coupling is controlled at the level of the cross-bridge, the kinetics of which are governed by properties inherent to myofilaments themselves (Milani-Nejad et al., 2016). This is further supported by experiments in which the cross-bridge is perturbed after the contraction period. A small-amplitude vibration (Janssen et al., 1996) or a small fast stretch (Chung et al., 2017) at or after twitch peak force development changes the cross-bridge cycling and accelerates the relaxation of the twitch, uncoupling relaxation from contraction.

cMyBP-C has previously been shown to interact with the thin filament in a phosphorylation-dependent manner (Pfuhl and Gautel, 2012; Shaffer et al., 2009), the S2 region of the myosin heavy chain also in a phosphorylation-dependent manner (Gruen et al., 1999), the S1-S2 hinge region of myosin (Ababou et al., 2008), the regulatory light chain of the S1 region of myosin heavy chain (Ratti et al., 2011), titin (Freiburg and Gautel, 1996), the LMM region of myosin (Flashman et al., 2007; Miyamoto et al., 1999), and to other cMyBP-C molecules (C5–C7 region of one to the C8–C10 of another; Moolman-Smook et al., 2002). The interactions of the C1mC2 region in particular have been shown to play important roles in cross-bridge formation and cycling (Weisberg and Winegrad, 1996), making cross-bridges more likely to form (modulated by Ca^{2+}) and cycle in response to the same activators that modulate contraction. We therefore believe that it may be cMyBP-C that impacts contraction and relaxation rates.

In conclusion, the results of the present study demonstrate that CR coupling is unaffected by cardiac remodeling resulting from prolonged exercise training and/or permanent cardiac injury in the canine model. Although we cannot yet make the distinction that CR coupling is a fundamental property of the myocardium, based on the available literature, we believe cMyBP-C may play a key role. Additional studies that investigate CR-coupling mechanisms at the cross-bridge level will shed more light on this relationship and how it goes awry in disease, and ultimately lead to improved patient care.

Acknowledgments

Henk L. Granzier served as editor.

This study was supported by National Heart, Lung, and Blood Institute grants R01-HL-068609 and HL-086700 (to G.E. Billman).

The authors declare no competing financial interests.

Author contributions: J.J. Santini Gonzalez, S.J. Repas, B.D. Canan, and P.M.L. Janssen performed experiments; F. Fazlollahi, J.J. Santini Gonzalez, S.J. Repas, B.D. Canan, and P.M.L. Janssen analyzed data; G.E. Billman performed surgical preparation and supervised the exercise training of the animals; F. Fazlollahi and P.M.L. Janssen prepared figures; F. Fazlollahi, G.E. Billman, and P.M.L. Janssen edited and revised the manuscript; F. Fazlollahi, J.J. Santini Gonzalez, S.J. Repas, B.D. Canan, and P.M.L. Janssen approved the final version of the manuscript; G.E. Billman and P.M.L. Janssen interpreted results of the experiments; G.E. Billman and P.M.L. Janssen conceived and designed the research; and F. Fazlollahi drafted the manuscript.

Submitted: 18 November 2020
Revised: 20 February 2021
Accepted: 18 March 2021

References

Ababou, A., E. Rostkova, S. Mistry, C. Le Masurier, M. Gautel, and M. Pfuhl. 2008. Myosin binding protein C positioned to play a key role in regulation of muscle contraction: structure and interactions of domain C1. *J. Mol. Biol.* 384:615–630. https://doi.org/10.1016/j.jmb.2008.09.065

Allen, D.G., and S. Kurihara. 1979. Calcium transients at different muscle lengths in rat ventricular muscle [proceedings]. *J. Physiol.* 292:68P–69P.

Anversa, P., G. Olivetti, and J.M. Capasso. 1991. Cellular basis of ventricular remodeling after myocardial infarction. *Am. J. Cardiol.* 68:7D–16D. https://doi.org/10.1016/0002-9149(91)90256-K

Babu, G.J., P. Bhupathy, N.N. Petrashevskaya, H. Wang, S. Raman, D. Wheeler, G. Jagatheesan, D. Wieczorek, A. Schwartz, P.M.L. Janssen, et al. 2006. Targeted overexpression of sarcolipin in the mouse heart decreases sarcoplasmic reticulum calcium transport and cardiac contractility. *J. Biol. Chem.* 281:3972–3979. https://doi.org/10.1074/jbc.M508998200

Backx, P.H., W.D. Gao, M.D. Azan-Backx, and E. Marban. 1995. The relationship between contractile force and intracellular [Ca2+] in intact rat cardiac trabeculae. *J. Gen. Physiol.* 105:1–19. https://doi.org/10.1085/jgp.105.1.1

Bertero, E., and C. Maack. 2018. Metabolic remodelling in heart failure. *Nat. Rev. Cardiol.* 15:457–470. https://doi.org/10.1038/s41569-018-0044-6

Billman, G.E. 2005. In-vivo models of arrhythmias: A canine model of sudden cardiac death. *In* Dhein, S., F.W. Mohr, and M. Delmar, eds. Practical Methods in Cardiovascular Research. Springer-Verlag, Berlin, Heidelberg. 111–128. https://doi.org/10.1007/3-540-26574-0_7

Billman, G.E. 2006. A comprehensive review and analysis of 25 years of data from an in vivo canine model of sudden cardiac death: implications for future anti-arrhythmic drug development. *Pharmacol. Ther.* 111:808–835. https://doi.org/10.1016/j.pharmthera.2006.01.002

Billman, G.E., and W.S. Harris. 2011. Effect of dietary omega-3 fatty acids on the heart rate and the heart rate variability responses to myocardial ischemia or submaximal exercise. *Am. J. Physiol. Heart Circ. Physiol.* 300:H2288–H2299. https://doi.org/10.1152/ajpheart.00140.2011

Billman, G.E., and M. Kukielka. 2006. Effects of endurance exercise training on heart rate variability and susceptibility to sudden cardiac death: protection is not due to enhanced cardiac vagal regulation. *J Appl Physiol (1985).* 100:896–906. https://doi.org/10.1152/japplphysiol.01328.2005

Billman, G.E., and M. Kukielka. 2007. Effect of endurance exercise training on heart rate onset and heart rate recovery responses to submaximal exercise in animals susceptible to ventricular fibrillation. *J Appl Physiol (1985).* 102:231–240. https://doi.org/10.1152/japplphysiol.00793.2006

Billman, G.E., and M. Kukielka. 2008. Novel transient outward and ultra-rapid delayed rectifier current antagonist, AVE0118, protects against ventricular fibrillation induced by myocardial ischemia. *J. Cardiovasc. Pharmacol.* 51:352–358. https://doi.org/10.1097/FJC.0b013e31816586bd

Billman, G.E., K.L. Cagnoli, T. Csepe, N. Li, P. Wright, P.J. Mohler, and V.V. Fedorov. 2015. Exercise training-induced bradycardia: evidence for enhanced parasympathetic regulation without changes in intrinsic sinoatrial node function. *J Appl Physiol (1985).* 118:1344–1355. https://doi.org/10.1152/japplphysiol.01111.2014

Billman, G.E., M. Kukielka, R. Kelley, M. Moustafa-Bayoumi, and R.A. Altschuld. 2006. Endurance exercise training attenuates cardiac β2-adrenoceptor responsiveness and prevents ventricular fibrillation in animals susceptible to sudden death. *Am. J. Physiol. Heart Circ. Physiol.* 290:H2590–H2599. https://doi.org/10.1152/ajpheart.01220.2005

Billman, G.E., Y. Nishijima, A.E. Belevych, D. Terentyev, Y. Xu, K.M. Haizlip, M.M. Monasky, N. Hiranandani, W.S. Harris, S. Gyorke, et al. 2010. Effects of dietary omega-3 fatty acids on ventricular function in dogs with healed myocardial infarctions: in vivo and in vitro studies. *Am. J. Physiol. Heart Circ. Physiol.* 298:H1219–H1228. https://doi.org/10.1152/ajpheart.01065.2009

Bonilla, I.M., A.E. Belevych, A. Sridhar, Y. Nishijima, H.T. Ho, Q. He, M. Kukielka, D. Terentyev, R. Terentyeva, B. Liu, et al. 2012. Endurance exercise training normalizes repolarization and calcium-handling abnormalities, preventing ventricular fibrillation in a model of sudden cardiac death. *J Appl Physiol (1985).* 113:1772–1783. https://doi.org/10.1152/japplphysiol.00175.2012

Borlaug, B.A., and D.A. Kass. 2008. Ventricular-vascular interaction in heart failure. *Heart Fail. Clin.* 4:23–36. https://doi.org/10.1016/j.hfc.2007.10.001

Canan, B.D., K.M. Haizlip, Y. Xu, M.M. Monasky, N. Hiranandani, N. Milani-Nejad, K.D. Varian, J.L. Slabaugh, E.J. Schultz, V.V. Fedorov, et al. 2016. Effect of exercise training and myocardial infarction on force development and contractile kinetics in isolated canine myocardium. *J Appl Physiol (1985).* 120:817–824. https://doi.org/10.1152/japplphysiol.00775.2015

Chung, C.S., C.W. Hoopes, and K.S. Campbell. 2017. Myocardial relaxation is accelerated by fast stretch, not reduced afterload. *J. Mol. Cell. Cardiol.* 103:65–73. https://doi.org/10.1016/j.yjmcc.2017.01.004

Craig, R., and G. Offer. 1976. The location of C-protein in rabbit skeletal muscle. *Proc. R. Soc. Lond. B Biol. Sci.* 192:451–461. https://doi.org/10.1098/rspb.1976.0023

Dorhout Mees, E.J. 2013. Diastolic heart failure: a confusing concept. *Heart Fail. Rev.* 18:503–509. https://doi.org/10.1007/s10741-012-9344-9

Flashman, E., H. Watkins, and C. Redwood. 2007. Localization of the binding site of the C-terminal domain of cardiac myosin-binding protein-C on the myosin rod. *Biochem. J.* 401:97–102. https://doi.org/10.1042/BJ20060500

Freiburg, A., and M. Gautel. 1996. A molecular map of the interactions between titin and myosin-binding protein C. Implications for sarcomeric assembly in familial hypertrophic cardiomyopathy. *Eur. J. Biochem.* 235:317–323. https://doi.org/10.1111/j.1432-1033.1996.00317.x

Gautel, M., O. Zuffardi, A. Freiburg, and S. Labeit. 1995. Phosphorylation switches specific for the cardiac isoform of myosin binding protein-C: a modulator of cardiac contraction? *EMBO J.* 14:1952–1960. https://doi.org/10.1002/j.1460-2075.1995.tb07187.x

Gielen, S., M.H. Laughlin, C. O'Conner, and D.J. Duncker. 2015. Exercise training in patients with heart disease: review of beneficial effects and clinical recommendations. *Prog. Cardiovasc. Dis.* 57:347–355. https://doi.org/10.1016/j.pcad.2014.10.001

Gruen, M., H. Prinz, and M. Gautel. 1999. cAPK-phosphorylation controls the interaction of the regulatory domain of cardiac myosin binding protein C with myosin-S2 in an on-off fashion. *FEBS Lett.* 453:254–259. https://doi.org/10.1016/S0014-5793(99)00727-9

Heling, L.W.H.J., M.A. Geeves, and N.M. Kad. 2020. MyBP-C: one protein to govern them all. *J. Muscle Res. Cell Motil.* 41:91–101. https://doi.org/10.1007/s10974-019-09567-1

Hiranandani, N., G.E. Billman, and P.M.L. Janssen. 2010. Effects of hydroxyl radical induced-injury in atrial versus ventricular myocardium of dog and rabbit. *Front. Physiol.* 1:25. https://doi.org/10.3389/fphys.2010.00025

Hiranandani, N., S. Raman, A. Kalyanasundaram, M. Periasamy, and P.M.L. Janssen. 2007. Frequency-dependent contractile strength in mice over- and underexpressing the sarco(endo)plasmic reticulum calcium-ATPase. *Am. J. Physiol. Regul. Integr. Comp. Physiol.* 293:R30–R36. https://doi.org/10.1152/ajpregu.00508.2006

Janssen, P.M.L. 2010. Myocardial contraction-relaxation coupling. *Am. J. Physiol. Heart Circ. Physiol.* 299:H1741–H1749. https://doi.org/10.1152/ajpheart.00759.2010

Janssen, P.M.L. 2019. Myocardial relaxation in human heart failure: Why sarcomere kinetics should be center-stage. *Arch. Biochem. Biophys.* 661:145–148. https://doi.org/10.1016/j.abb.2018.11.011

Janssen, P.M.L., and M. Periasamy. 2007. Determinants of frequency-dependent contraction and relaxation of mammalian myocardium. *J. Mol. Cell. Cardiol.* 43:523–531. https://doi.org/10.1016/j.yjmcc.2007.08.012

Janssen, P.M.L., N. Hiranandani, T.A. Mays, and J.A. Rafael-Fortney. 2005. Utrophin deficiency worsens cardiac contractile dysfunction present in dystrophin-deficient mdx mice. *Am. J. Physiol. Heart Circ. Physiol.* 289:H2373–H2378. https://doi.org/10.1152/ajpheart.00448.2005

Janssen, P.M.L., H. Honda, Y. Koiwa, and K. Shirato. 1996. The effect of diastolic vibration on the relaxation of rat papillary muscle. *Cardiovasc. Res.* 32:344–350. https://doi.org/10.1016/0008-6363(96)00094-6

Janssen, P.M.L., L.B. Stull, and E. Marbán. 2002. Myofilament properties comprise the rate-limiting step for cardiac relaxation at body temperature in the rat. *Am. J. Physiol. Heart Circ. Physiol.* 282:H499–H507. https://doi.org/10.1152/ajpheart.00595.2001

Janssen, P.M.L., B.J. Biesiadecki, M.T. Ziolo, and J.P. Davis. 2016. The need for speed: Mice, men, and myocardial kinetic reserve. *Circ. Res.* 119:418–421. https://doi.org/10.1161/CIRCRESAHA.116.309126

Jones, W.K., I.L. Grupp, T. Doetschman, G. Grupp, H. Osinska, T.E. Hewett, G. Boivin, J. Gulick, W.A. Ng, and J. Robbins. 1996. Ablation of the murine α

myosin heavy chain gene leads to dosage effects and functional deficits in the heart. *J. Clin. Invest.* 98:1906–1917. https://doi.org/10.1172/JCI118992

Kessler, E.L., M. Boulaksil, H.V.M. van Rijen, M.A. Vos, and T.A.B. van Veen. 2014. Passive ventricular remodeling in cardiac disease: focus on heterogeneity. *Front. Physiol.* 5:482. https://doi.org/10.3389/fphys.2014.00482

Kukielka, M., B.J. Holycross, and G.E. Billman. 2011. Endurance exercise training reduces cardiac sodium/calcium exchanger expression in animals susceptible to ventricular fibrillation. *Front. Physiol.* 2:3. https://doi.org/10.3389/fphys.2011.00003

Loukianov, E., Y. Ji, I.L. Grupp, D.L. Kirkpatrick, D.L. Baker, T. Loukianova, G. Grupp, J. Lytton, R.A. Walsh, and M. Periasamy. 1998. Enhanced myocardial contractility and increased Ca2+ transport function in transgenic hearts expressing the fast-twitch skeletal muscle sarcoplasmic reticulum Ca2+-ATPase. *Circ. Res.* 83:889–897. https://doi.org/10.1161/01.RES.83.9.889

Luther, P.K., H. Winkler, K. Taylor, M.E. Zoghbi, R. Craig, R. Padrón, J.M. Squire, and J. Liu. 2011. Direct visualization of myosin-binding protein C bridging myosin and actin filaments in intact muscle. *Proc. Natl. Acad. Sci. USA.* 108:11423–11428. https://doi.org/10.1073/pnas.1103216108

Ma, Y., L.E. de Castro Brás, H. Toba, R.P. Iyer, M.E. Hall, M.D. Winniford, R.A. Lange, S.C. Tyagi, and M.L. Lindsey. 2014. Myofibroblasts and the extracellular matrix network in post-myocardial infarction cardiac remodeling. *Pflugers Arch.* 466:1113–1127. https://doi.org/10.1007/s00424-014-1463-9

Mannozzi, J., L. Massoud, J. Kaur, M. Coutsos, and D.S. O'Leary. 2020. Ventricular contraction and relaxation rates during muscle metaboreflex activation in heart failure: are they coupled? *Exp. Physiol.* 106:401–411. https://doi.org/10.1113/EP089053

Milani-Nejad, N., J.H. Chung, B.D. Canan, J.P. Davis, V.V. Fedorov, R.S.D. Higgins, A. Kilic, P.J. Mohler, and P.M.L. Janssen. 2016. Insights into length-dependent regulation of cardiac cross-bridge cycling kinetics in human myocardium. *Arch. Biochem. Biophys.* 601:48–55. https://doi.org/10.1016/j.abb.2016.02.005

Milani-Nejad, N., Y. Xu, J.P. Davis, K.S. Campbell, and P.M.L. Janssen. 2013. Effect of muscle length on cross-bridge kinetics in intact cardiac trabeculae at body temperature. *J. Gen. Physiol.* 141:133–139. https://doi.org/10.1085/jgp.201210894

Miyamoto, C.A., D.A. Fischman, and F.C. Reinach. 1999. The interface between MyBP-C and myosin: site-directed mutagenesis of the CX myosin-binding domain of MyBP-C. *J. Muscle Res. Cell Motil.* 20:703–716. https://doi.org/10.1023/A:1005513312939

Monasky, M.M., K.D. Varian, J.P. Davis, and P.M.L. Janssen. 2008. Dissociation of force decline from calcium decline by preload in isolated rabbit myocardium. *Pflugers Arch.* 456:267–276. https://doi.org/10.1007/s00424-007-0394-0

Moolman-Smook, J., E. Flashman, W. de Lange, Z. Li, V. Corfield, C. Redwood, and H. Watkins. 2002. Identification of novel interactions between domains of myosin binding protein-C that are modulated by hypertrophic cardiomyopathy missense mutations. *Circ. Res.* 91:704–711. https://doi.org/10.1161/01.RES.0000036750.81083.83

Palmer, B.M., D. Georgakopoulos, P.M. Janssen, Y. Wang, N.R. Alpert, D.F. Belardi, S.P. Harris, R.L. Moss, P.G. Burgon, C.E. Seidman, et al. 2004. Role of cardiac myosin binding protein C in sustaining left ventricular systolic stiffening. *Circ. Res.* 94:1249–1255. https://doi.org/10.1161/01.RES.0000126898.95550.31

Periasamy, M., T.D. Reed, L.H. Liu, Y. Ji, E. Loukianov, R.J. Paul, M.L. Nieman, T. Riddle, J.J. Duffy, T. Doetschman, et al. 1999. Impaired cardiac performance in heterozygous mice with a null mutation in the sarco(endo) plasmic reticulum Ca2+-ATPase isoform 2 (SERCA2) gene. *J. Biol. Chem.* 274:2556–2562. https://doi.org/10.1074/jbc.274.4.2556

Pfuhl, M., and M. Gautel. 2012. Structure, interactions and function of the N-terminus of cardiac myosin binding protein C (MyBP-C): who does what, with what, and to whom? *J. Muscle Res. Cell Motil.* 33:83–94. https://doi.org/10.1007/s10974-012-9291-z

Ratti, J., E. Rostkova, M. Gautel, and M. Pfuhl. 2011. Structure and interactions of myosin-binding protein C domain C0: cardiac-specific regulation of myosin at its neck? *J. Biol. Chem.* 286:12650–12658. https://doi.org/10.1074/jbc.M110.156646

Risi, C., B. Belknap, E. Forgacs-Lonart, S.P. Harris, G.F. Schröder, H.D. White, and V.E. Galkin. 2018. N-terminal domains of cardiac myosin binding protein C cooperatively activate the thin filament. *Structure.* 26:1604–1611.e4. https://doi.org/10.1016/j.str.2018.08.007

Ritzer, T.F., A.A. Bove, and R.A. Carey. 1980. Left ventricular performance characteristics in trained and sedentary dogs. *J. Appl. Physiol.* 48:130–138. https://doi.org/10.1152/jappl.1980.48.1.130

Savarese, G., and L.H. Lund. 2017. Global public health burden of heart failure. *Card. Fail. Rev.* 3:7–11. https://doi.org/10.15420/cfr.2016:25:2

Shaffer, J.F., R.W. Kensler, and S.P. Harris. 2009. The myosin-binding protein C motif binds to F-actin in a phosphorylation-sensitive manner. *J. Biol. Chem.* 284:12318–12327. https://doi.org/10.1074/jbc.M808850200

Stull, L.B., N. Hiranandani, M.A. Kelley, M.K. Leppo, E. Marbán, and P.M.L. Janssen. 2006. Murine strain differences in contractile function are temperature- and frequency-dependent. *Pflugers Arch.* 452:140–145. https://doi.org/10.1007/s00424-005-0020-y

Stull, L.B., M.K. Leppo, E. Marbán, and P.M.L. Janssen. 2002. Physiological determinants of contractile force generation and calcium handling in mouse myocardium. *J. Mol. Cell. Cardiol.* 34:1367–1376. https://doi.org/10.1006/jmcc.2002.2065

Stypmann, J., P.M.L. Janssen, J. Prestle, M.A. Engelen, H. Kögler, R. Lüllmann-Rauch, L. Eckardt, K. von Figura, J. Landgrebe, A. Mleczko, and P. Saftig. 2006. LAMP-2 deficient mice show depressed cardiac contractile function without significant changes in calcium handling. *Basic Res. Cardiol.* 101:281–291. https://doi.org/10.1007/s00395-006-0591-6

Vega, R.B., J.P. Konhilas, D.P. Kelly, and L.A. Leinwand. 2017. Molecular mechanisms underlying cardiac adaptation to exercise. *Cell Metab.* 25:1012–1026. https://doi.org/10.1016/j.cmet.2017.04.025

Weber, K.T., R. Pick, M.A. Silver, G.W. Moe, J.S. Janicki, I.H. Zucker, and P.W. Armstrong. 1990. Fibrillar collagen and remodeling of dilated canine left ventricle. *Circulation.* 82:1387–1401. https://doi.org/10.1161/01.CIR.82.4.1387

Weisberg, A., and S. Winegrad. 1996. Alteration of myosin cross bridges by phosphorylation of myosin-binding protein C in cardiac muscle. *Proc. Natl. Acad. Sci. USA.* 93:8999–9003. https://doi.org/10.1073/pnas.93.17.8999

Yasuda, M., S. Koshida, N. Sato, and T. Obinata. 1995. Complete primary structure of chicken cardiac C-protein (MyBP-C) and its expression in developing striated muscles. *J. Mol. Cell. Cardiol.* 27:2275–2286. https://doi.org/10.1016/S0022-2828(95)91731-4